

Study on poly(vinylidene fluoride)/nickel composites with low percolation

R. K. Goyal*, R. Sulakhe

Department of Metallurgy and Materials Science, College of Engineering, Shivajinagar, Pune 411005, India

*Corresponding author. Tel: (+91) 20 25507275; E-mail: rkgoyal72@yahoo.co.in

Received: 28 August 2014, Revised: 20 November 2014 and Accepted: 27 November 2014

ABSTRACT

The preparation, electrical and thermal properties of nickel (Ni) particles filled poly(vinylidene fluoride) (PVDF) composites were discussed in this paper. The experimental density of the composites was close to that of theoretical density. X-ray diffraction (XRD) and Fourier transform infrared spectroscopy (FTIR) showed that PVDF has primarily α -phase. The coefficient of thermal expansion of the composites decreased approximately 30 % compared to pure PVDF. The percolation threshold of the composite is about 5 vol% Ni, which is less than one-third of the value reported for metal filled polymer composites in the literature. The significantly lower percolation was attributed to the increased crystallinity and the better processing method which results in an easy formation of 3-dimensional network of Ni particles in the matrix, as confirmed by scanning electron microscopy (SEM). The electrical conductivity of these composites increased from 6.3×10^{-13} S/cm to 2.6×10^{-1} S/cm which is better and comparable than those of required for antistatic (10^{-4} - 10^{-8} S/cm) and electromagnetic interference (EMI) shielding applications. The significant increase in electrical and thermal properties showed that these composites might be potential candidates for the EMI shielding and antistatic devices. Copyright © 2015 VBRI press.

Keywords: Polymer-matrix composites; electrical properties; thermal properties; electron microscopy.



Rajendra Kumar Goyal received Ph.D. in Materials Science from the Indian Institute of Technology Bombay, Mumbai, India in 2007. He was awarded Best Ph.D. Thesis Prize in Materials Science for the year 2007 by the Materials Research Society of India (MRSI). He obtained B.E. in Metallurgical Engineering from Malviya Regional Engineering College (now, NIT) Jaipur, University of Rajasthan, India in 1996. Presently, he is an Associate Professor in the Department of Metallurgy and Materials Science, College of Engineering,

Pune (COEP), India. He also has research and industrial experience of more than 12 years. He has published over 100 papers in national and international peer-reviewed journals and conferences. He is a member of editorial board and reviewer of many international journals. He has successfully completed several research projects funded by funding agencies like ISRO, UGC, AICTE, India. His main research area is polymer composites/nanocomposites, nanomaterials, characterization of materials, electronic materials, structure-properties relationship etc.



Rishika Sulakhe obtained M. Tech. in Physical Metallurgy from Department of Metallurgy and Materials Science, College of Engineering, Pune, India in 2012. She obtained B.Tech. degree in Metallurgical Engineering, from National Institute of Technology, Raipur in 2010. She joined the Department of Mechanical Engineering, Dr. D.Y. Patil School of Engineering, Pune, India as Assistant Professor in 2012. Her interesting research area is polymer matrix micro-and nanocomposites.

Introduction

The rapid development of electronic devices and as a consequence of the rise of electrostatic discharge (ESD), electromagnetic interference (EMI) and radio frequency interference (RFI), the development of new electrically conductive polymer based composites are in demand to prevent devastating effects on the quality and reliability of manufactured electronics equipments. The EMI is the electronic disturbance which interrupts, degrade or limit the effective performance of electronic devices. Therefore, protection of devices and circuits against EMI with shielded materials has become an essential issue. The shielded materials must possess good electrical conductivity, which can be achieved by adding appropriate volume fraction of metals like silver (Ag), copper (Cu), aluminum (Al), nickel (Ni), iron (Fe) or conductive particles such as carbon black (CB), carbon fiber (CF) and steel filaments to the polymer matrix [1-3]. In metal-polymer composites, there is a drastic increase in the electrical conductivity over a narrow range of volume fraction of the conductive fillers. This sudden increase in the conductivity is due to the formation of 3-dimensional network of the conductive filler in the matrix. This phenomenon is called percolation [4] and the minimum volume fraction of the conductive filler at which drastic increase in electrical conductivity occurs is called percolation threshold. The percolation threshold depends

upon the size, shape and aspect ratio of the fillers, processing method, adhesion between the fillers and the matrix, and the spatial arrangement of the fillers in the matrix. Depending upon these factors, the percolation threshold varies from 2 to 57 vol% [1-6] for metal filled polymer composites. It decreases with increasing aspect ratio of the fillers. The efficiency of the 3-dimensional network formation for the fillers is inversely proportional to the packing density of the filler [7, 8] and polymer crystallinity [9]. It is well known that the structure of the crystalline region is highly dense, whereas that of the amorphous region is quite loose. Therefore, conductive fillers can be dispersed preferably in the amorphous region of the matrix. For example, the percolation threshold for the Fe filled high density polyethylene (HDPE) (crystallinity ~ 68 %) and low density polyethylene (LDPE) (crystallinity ~ 34 %) composites is 14-15 vol% and 12-20 vol%, respectively [9].

Poly(vinylidene fluoride) (PVDF) is a semi-crystalline polymer which has good mechanical properties, good chemical resistance and excellent processability. It has a continuous use temperature of about 150 °C [10]. It is electrically insulator. Its electrical conductivity has been increased by the addition of various fillers like Ni [5-6], graphite [11] and CB [12]. Xu and Dang et al. [13] studied the effect of CB, Ni, Zinc (Zn) and tungsten (W) on electrical conductivity of PVDF. They found that the percolation threshold for PVDF/CB, PVDF/Ni, PVDF/W and PVDF/Zn was about 8, 15, 22 and 27 vol%, respectively. Though, CB/PVDF composite showed lowest percolation threshold but its value increases when fluorinated-CB was used as filler [14]. According to Panda et al. [5-6] the percolation threshold for PVDF/Ni micro- and nanocomposites was about 57 vol% [5] and 28 vol% [6], respectively. These values are very high compared to the theoretical and experimental values. Second, the electrical conductivity increased approximately 3 orders of magnitude, i.e., from 1.0×10^{-9} S/cm for pure PVDF to 1.0×10^{-6} S/cm for 57 vol% composite [5]. In contrast, according to Xu and Dang [13], the maximum conductivity achieved for PVDF/Ni composites was about 3×10^{-4} S/cm. Nevertheless, the percolation threshold should be as low as possible to minimize loss in mechanical properties and flexibility of the composites. For example, the elongation and tensile strength of polyimide siloxane/Ni composites decreased significantly above 12 vol% Ni content compared to the composites containing lower Ni content [15]. Unfortunately, a systematic study on thermal and structural properties of PVDF/Ni composites was not carried out to explain the improvement in electrical conductivity, yet. Probably, these properties could have answered the reason of high percolation threshold (15-57 vol%). Moreover, owing to high absorption coefficient and low reflection coefficient, Ni has been widely used as filler for the EMI shielded polymeric materials. The Ni has electrical conductivity of 1.3×10^5 S/cm and relative magnetic permeability of 100 [16, 17].

In view of above, the aim of this study is to increase the electrical conductivity of the PVDF/Ni composites with a lower percolation threshold (i.e., 5 vol%) compared to the values reported in the literature [5, 6]. Novelty of the process reported herein involved the use of ultrasonic bath

during mechanical stirring of Ni particles in a solution of PVDF/DMAc. This results in better dispersion of Ni particles throughout the PVDF matrix. Further to avoid settling of Ni particles, a series of thin composite films containing 0-70 wt% (0-32 vol%) micron sized Ni powder was prepared using (2 times) hot pressing. The resultant composites showed a low percolation threshold and the obtained films have good flexibility, dimensional stability and thermal stability. Prepared composites were characterized for crystal structure, morphology, electrical conductivity, thermal stability and dimensional stability (coefficient of thermal expansion) using x-ray diffraction, scanning electron microscopy (SEM), high resistivity meter/7½ digit digital multimeter, thermo gravimetric analyzer (TGA)/differential scanning calorimetry (DSC), and thermomechanical analyzer, respectively.

Experimental

Materials

Commercial grade PVDF granule was procured from Pennwalt India, Mumbai and N,N-dimethyl acetamide (DMAc) (99.8% pure, HPLC grade) was used as solvent medium. The micro sized Ni powder (99.8 % trace metal, Sigma Aldrich Co., USA) was used in as received condition. According to supplier, the particle size of Ni powder was 5 µm. The differential particle size distribution of Ni powder was determined on Nicomp 380 Particle Size Analyser using the standard test method reported in our previous paper [2]. As can be seen from the Fig. 1, Ni particle size ranges from 0.6 µm to 1.2 µm with mean particle size of 0.9 µm. Fig. 2 shows the typical SEM micrograph of Ni powder.

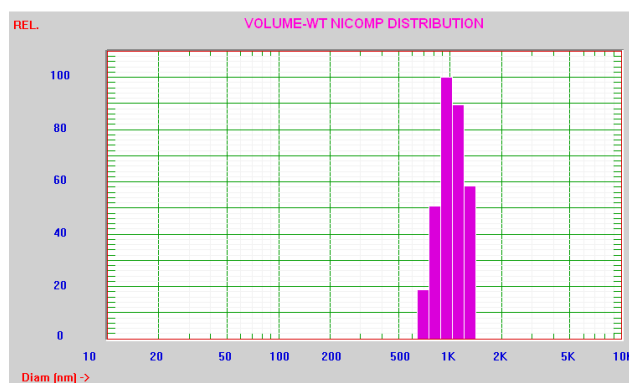


Fig. 1. Differential particle size distribution of micro-Ni powder.

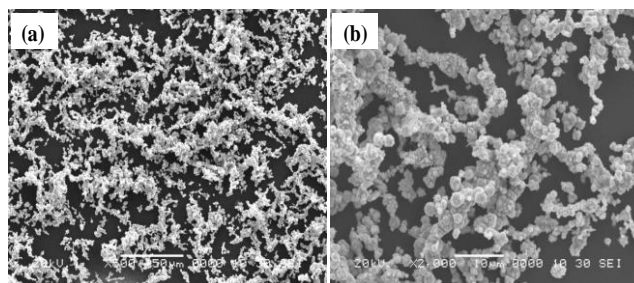


Fig. 2. SEM images of micro-Ni powder at magnifications of (a) 500× and (b) 2000×.

It can be seen from the **Fig. 2** that the Ni particles are in aggregated form having dendrites like shape. The size of each dendrite varies from few to several tens of microns. It also seems that each dendrite consists of several isolated non-spherical particles which are bounded together due to van der Waals forces.

Fabrication of PVDF/Ni composite

Both PVDF and Ni powders were dried in a vacuum oven and weighted in an appropriate quantity. To break the aggregates of Ni particles, it was suspended in DMAc solvent using ultrasonic bath for 30 min. The PVDF were added to the Ni/DMAc suspension and the solution was mixed and heated for 5h using mechanical stirrer at speed of 500 rpm to get viscous solution. Then, the viscous solution was poured on the glass plate to cast a thin film (<100 μm) in order to avoid settling of Ni particles. This film is dried at room temperature for 12-14 h and further dried in a vacuum oven (~ 500 mm Hg vacuum) at 150 $^{\circ}\text{C}$ for 6h. The dried films were cut into small pieces and filled into the steel die. The die-set was kept inside the heater and it was mounted on a compression molding machine. The sample was heated with heating rate of 10 $^{\circ}\text{C}/\text{min}$ under pressure (45 MPa) to a temperature of about 220 $^{\circ}\text{C}$. The dwell time was 45 min to ensure complete melting and consolidation of the powder. The sample was air cooled and then it was ejected after the die assembly reaches room temperature. For second repressing, this hot pressed sample was again repressed (for the pellets with lesser thicknesses) using the same processing parameter. The PVDF/Ni composites containing 0, 5, 10, 20, 30, 40, 50, 60 and 70 wt% Ni particles were fabricated using the above processing parameters and coded as C-0, C-5, C-10, C-20, C-30, C-40, C-50, C-60 and C-70, respectively. **Fig. 3** shows the schematic flow chart describing each processing steps clearly.

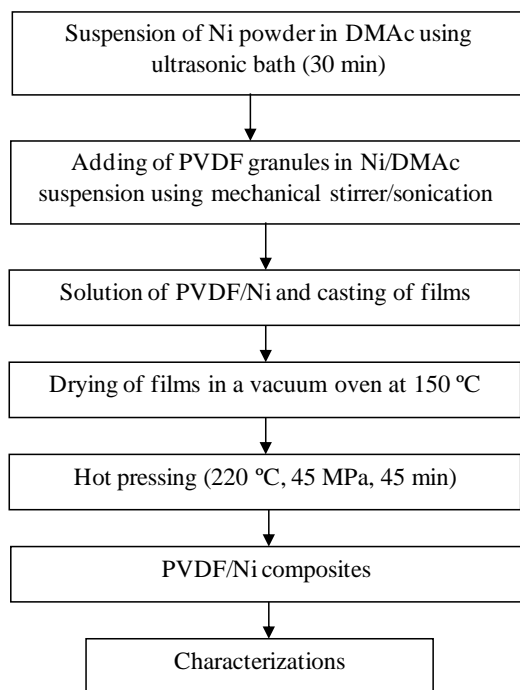


Fig. 3. Flow chart of the fabrication of PVDF/Ni composites.

Characterization of composites

Density: Theoretical density (ρ_{th}) of the composites was determined using rule of mixtures (ROM); $\rho_{\text{th}} = \rho_{\text{m}}(1-V_f) + \rho_f V_f$, where ρ_{m} is the density of the matrix (1.74 g/cm^3), ρ_f is the density of the Ni (8.9 g/cm^3), and V_f is the volume fraction of the Ni powder. For a given weight fraction of the Ni (W_f), the V_f was determined using Eq. (1) and specified in **Table 1**.

$$V_f = W_f / [W_f + (1 - W_f) \cdot (\rho_f / \rho_m)] \quad (1)$$

The experimental density (ρ_{exp}) of the composites was determined by the Archimedes Principle using Eq. (2).

$$\rho_{\text{exp}} = W_a \cdot \rho_l / (W_a - W_l) \quad (2)$$

where, ρ_l is the density of the medium (i.e., 0.79 g/cm^3 for ethanol), W_a is the weight of the composites in air and W_l is the weight of the composite in ethanol.

Table 1. Theoretical and experimental density of PVDF/Ni composites.

Sample Code	% Ni in PVDF matrix	
	By wt.	By vol.
C-0	0	0
C-10	10	2.17
C-20	20	4.76
C-30	30	7.89
C-40	40	11.76
C-50	50	16.66
C-60	60	23.07
C-70	70	31.81

Scanning electron microscopy (SEM)

Distribution of Ni particles across the cross section of the composites was analyzed using SEM (JEOL: JSM 6360A). For SEM analysis, surface of the polished samples was coated with a thin layer of platinum using sputter coater (JEOL: JEC 60) and mounted on metal stub which was grounded with a conductive adhesive aluminum tape to minimize the charging of the samples.

X-ray diffraction (XRD)

XRD patterns of pure Ni, PVDF and its composites containing 5 wt% (C-5) and 30 wt% Ni (C-30) were recorded on Phillips X'pert PANanalytical PW 3040/60. Ni filtered $\text{Cu } k_{\alpha}$ radiation ($\lambda=1.54 \text{ \AA}$) generated at 40 kV and 30 mA was used for angle (2θ) ranging from 10° to 60° . The scan step size and time per step was 0.02 and 5 s, respectively.

Fourier transform infra-red spectroscopy (FTIR)

FTIR spectra of pure PVDF (C-0) and 5 wt % (C-5) composite were recorded with a Perkin Elmer Spectrum 2000 FTIR spectrophotometer in the wave number range of

400-1000 cm^{-1} . The spectral resolution was 4 cm^{-1} . FTIR analysis was done in the transmission mode. Samples used were in the form of thin films having thickness of about 100 μm .

Thermal properties

The linear out-of-plane (through thickness direction) coefficient of thermal expansion (CTE) of the composites was determined using Perkin Elmer DMA 7e in thermo mechanical analyzer mode. A 100 mN force was applied to make the probe in good contact with sample. Before measuring CTE the samples were annealed at 160 $^{\circ}\text{C}$ for 2 h in a vacuum oven. Then the annealed sample was held under pressure for 5 min and heated to 150 $^{\circ}\text{C}$ at a heating rate of 5 $^{\circ}\text{C}/\text{min}$. The CTE (α) values were determined from the slope over specific temperature range of 50-100 $^{\circ}\text{C}$. The theoretical CTE (α_c) of the composites was calculated by the RoM using Eq. (3) [18].

$$\alpha_c = \alpha_m(1-V_f) + \alpha_f V_f \quad (3)$$

where, α_c , α_m , and α_f represent the linear CTE of composite, PVDF matrix and Ni filler, respectively.

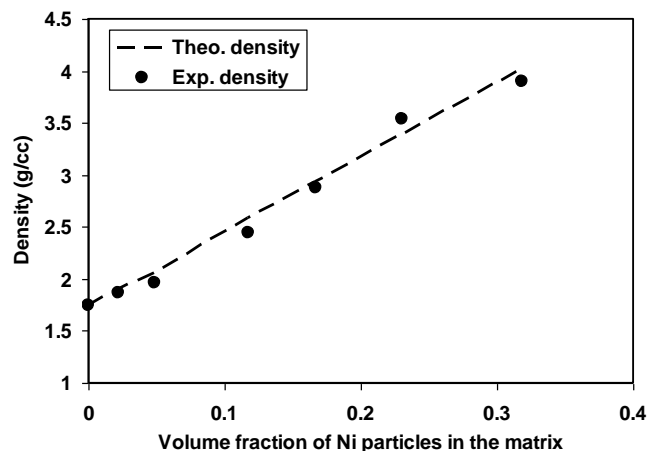


Fig. 4. Experimental and theoretical density of PVDF/Ni composite.

Differential scanning calorimetry (DSC) measurement was carried out to determine the thermal properties such as melting temperature (T_m), heat of crystallization (H_c), degree of crystallinity (χ_c), onset temperature of crystallization (T_{on}) and peak crystallization temperature (T_c) of the composites using DSC (TA Instruments: DSC Q10). The samples placed in an aluminum pan were first heated from 30 $^{\circ}\text{C}$ to 250 $^{\circ}\text{C}$ at a heating rate of 20 $^{\circ}\text{C}/\text{min}$ and soaked isothermally at 250 $^{\circ}\text{C}$ for 5 min to allow complete melting of the polymer. The samples were then cooled to - 50 $^{\circ}\text{C}$ at a cooling rate of 20 $^{\circ}\text{C}/\text{min}$. Each sample was subjected to double heating and cooling cycles under dry nitrogen (N_2) purge. The data of second heating and cooling were discussed. Thermo gravimetric analysis (TGA) measurement was done to find out the thermal stability and the percentage char yield of the composites using TGA (Universal Analysis 2000). The samples were heated from 50 $^{\circ}\text{C}$ to 800 $^{\circ}\text{C}$ at a heating rate of 20 $^{\circ}\text{C}/\text{min}$ in N_2 atmosphere. The maximum decomposition temperature (T_m) was taken as the temperature

corresponding to maximum of the peak obtained from the first order derivative curve of TGA (i.e., DTG). The % char yield was determined at temperature of 800 $^{\circ}\text{C}$.

Electrical properties

The dc electrical conductivity (σ_c) of the PVDF/Ni composites was determined at room temperature using; $\sigma_c = L/(R.A)$, where, R is the resistance (in ohms), L is the thickness (in cm) and A is the cross sectional area (in cm^2) of the composite sample. For its measurement, samples were coated with a thin layer of silver paste. The resistance of samples above 1 $\text{k}\Omega$ was measured using Electrometer (Keithley 6517B). The resistance below 1 $\text{k}\Omega$ was measured using 7½ digit digital multimeter (Keithley 2001).

Results and discussion

Density

Fig. 4 shows the experimental and theoretical density of the Ni filled PVDF composites. The experimental density of the composites increased with increasing content of Ni in the matrix. This is due to the higher density of Ni (8.9 g/cm^3) than the pure PVDF (1.74 g/cm^3). The experimental density of the composites is close to that of theoretical density which shows that the samples are almost porosity free. However, the density of the composites containing 32 vol% Ni is slightly (i.e., 3.46 %) lower than the theoretical density which may be due to the presence of voids resulted from aggregates of Ni particles.

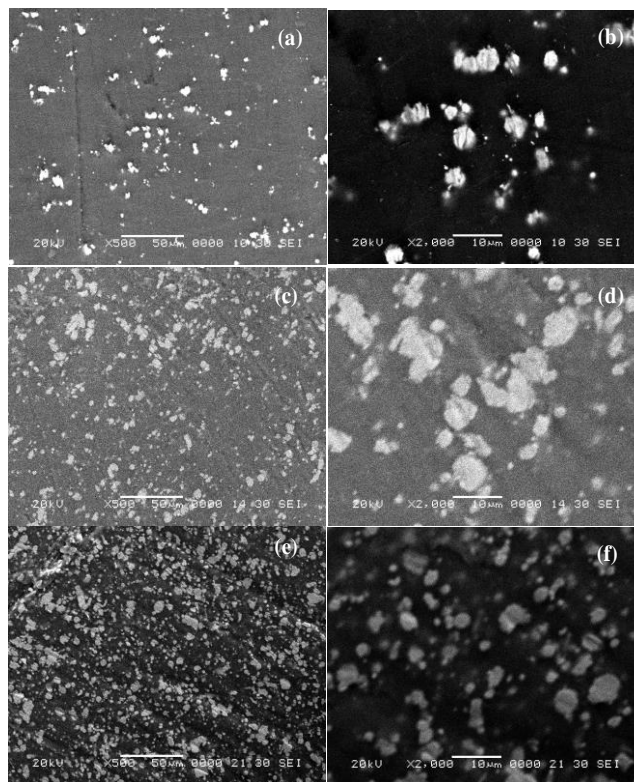


Fig. 5. SEM images of cross section of composites with (a and b) 10 wt% (C-10), (c and d) 40 wt% (C-40) and (e and f) 60 wt% (C-60) Ni at magnifications of 500 \times (a, c, & e) and 2000 \times (b, d, & f).

Scanning electron microscopy (SEM)

SEM was done to examine the nature of interface and the dispersion of Ni particles into the matrix. **Fig. 5** shows the SEM images of C-10, C-40, and C-60 composites at magnifications of 500× and 2000×. It can be seen from the **Fig. 5** that Ni particles are almost uniformly dispersed in the matrix. As the content of Ni increases, inter-particle distance decreases significantly, which results in a tendency to the formation of Ni aggregates at higher loading. In case of C-60 (**Fig. 5(e-f)**), the Ni particles are close enough to conduct the electrons by tunneling mechanism from a Ni particle to an adjacent Ni particle. Moreover, the Ni particles form a 3-dimensional conductive network in the matrix. It is interesting to see that there are no pores or voids in the C-60 composites. SEM images also revealed that the Ni particles are irregular in shape and formed chain-like structure (high structure), which could be one of the reasons of lower percolation threshold. At 70 wt% Ni (C-70) content, aggregates as well as primary Ni particles were observed in the matrix as shown in **Fig. 6**. These aggregates were probably formed due to the decreased inter-particle distances with increasing Ni content in the matrix. Moreover, thicker 3-dimensional conductive network (shown by dotted line in Fig. 6c) was observed compared to those of C-40 and C-60 composites. The critical inter-particle distance (CID) can be calculated using Eq. (4) [18].

$$CID = d \left[\left(\frac{\pi}{6 \cdot V_f} \right)^{1/3} - 1 \right] \quad (4)$$

where, d is the mean diameter (0.9 μm) of Ni particle as shown in Fig 1. From Eq. (4), it is clear that the CID decreases with increasing volume fraction of Ni for a given particle size. We found that the experimental CID was higher than those of theoretical one. This is also in agreement with the formation of Ni aggregates.

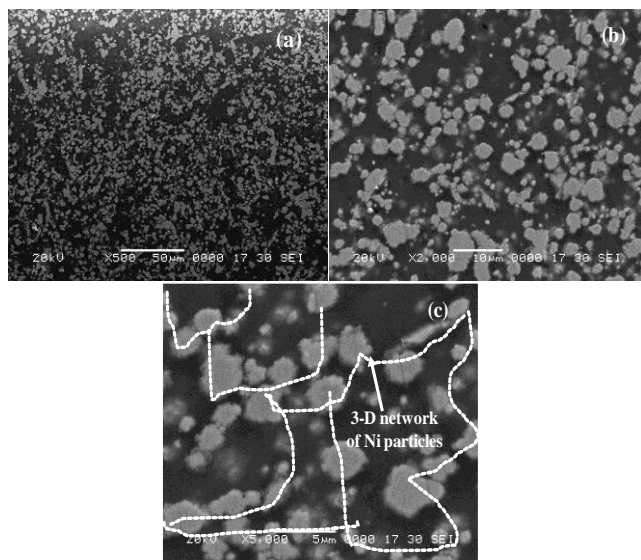


Fig. 6. SEM images of cross section of composite with 70 wt% Ni at magnifications of (a) 500×, (b) 2000× and (c) 5000×.

X-ray diffraction (XRD)

Fig. 7 shows XRD patterns for the Ni powder, pure PVDF and its composites containing 5 wt% (C-5) and 30 wt% Ni (C-30). Pure Ni powder showed diffraction peaks at 44.5°, 51.85° and 76.42° which correspond to the planes (111), (200) and (220), respectively, according to JCPDS file (PDF#040850). Pure PVDF showed prominent peaks at 18.5°, 20.2°, 26.8° and 39.3° which corresponds to the plane of (020), (110), (021) and (002), respectively [19-20], for α -phase of PVDF. However, peak at 18.5° indicates the presence of β -phase of PVDF. Both C-5 and C-30 composites showed the diffraction peaks of PVDF and Ni. It was also seen that as the Ni content increases, the 2 θ position of the PVDF diffraction peaks shifts towards higher angle slightly and thus, d-spacing of the lattice planes decreases. It indicates that the addition of Ni particle to the PVDF increases the crystallinity perfection, which is also confirmed from the DSC measurement.

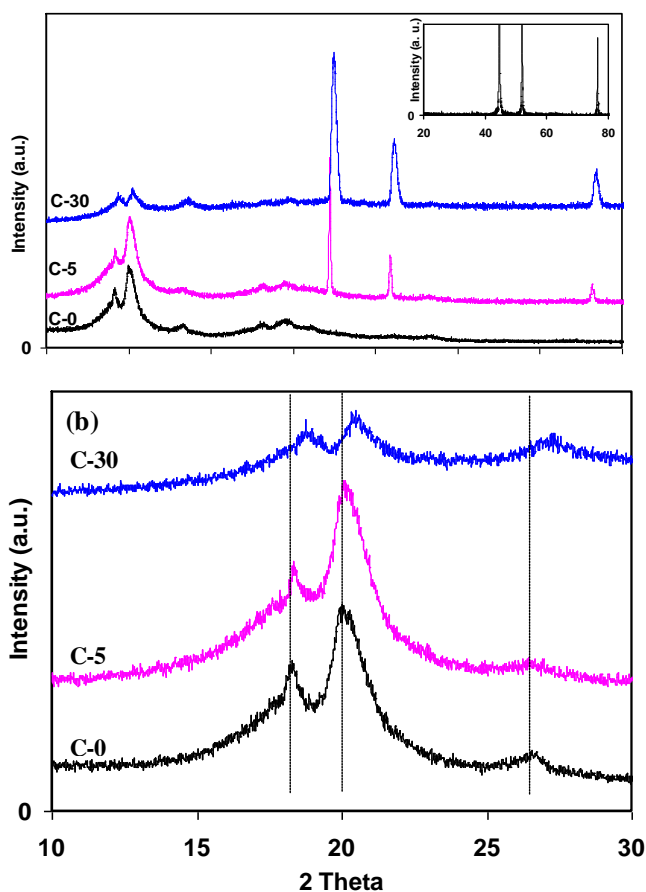


Fig. 7. (a) XRD patterns for the pure PVDF (C-0), 5 wt% (C-5), 30 wt% (C-30) Ni composites and (b) magnified XRD patterns indicating clearly the shifting of 2 θ peaks of PVDF. The inset of Fig. 7(a) shows the XRD of pure micro-Ni powder.

Fourier transform infrared (FTIR) spectroscopy

The presence of α -phase and/or β -phase of PVDF was confirmed using FTIR of the films of C-0 and C-5 composites. As shown in **Fig. 8**, C-0 showed sharp characteristic peaks at 531, 614, 764, 796, 852, and 976 cm^{-1} indicating presence of α -phase of PVDF, whereas characteristics peaks at 509 and 840 cm^{-1} showed the

presence of β -phase of PVDF [19-20]. In case of C-5, one additional peak at 430 cm^{-1} was found which indicates the presence of Ni in the composite [21]. However, the addition of Ni particles to the PVDF matrix did not enhance change from α to β -phase. In contrast, the addition of inorganic clay or processing method transforms the α -phase to β -phase [22].

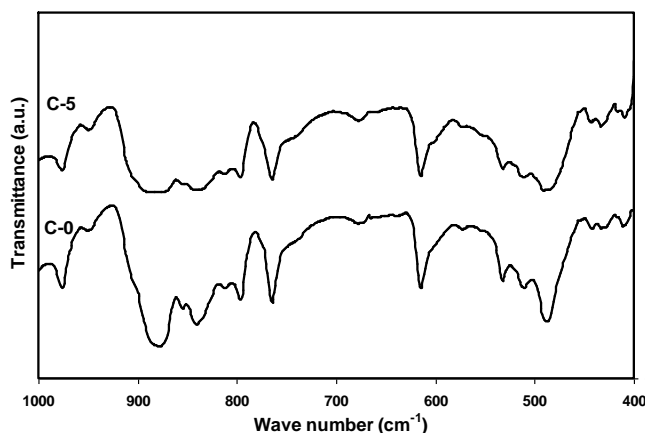


Fig. 8. FTIR spectra of pure PVDF(C-0) and 5 wt% (C-5) Ni composite.

Coefficient of thermal expansion (CTE)

The coefficient of thermal expansion (CTE) is used as a tool for evaluating the dimensional stability of the composites. Fig. 9 shows the experimental CTE of C-0, C-60 and C-70 composites. The value of thermal expansion of the composites increases non-linearly with increasing temperatures (not shown in Figure). The CTE values were calculated from the slope taken over specific temperature range of $50\text{--}100\text{ }^{\circ}\text{C}$. The CTE of pure PVDF was about $195 \times 10^{-6}\text{ }^{\circ}\text{C}^{-1}$ which is in close agreement with the value reported by Xu et al. [23]. It can be seen from the Fig. 9 that the CTE of C-70 (32 vol% Ni) composite decreased to a value of $136 \times 10^{-6}\text{ }^{\circ}\text{C}^{-1}$ which is 30% lower than that of pure PVDF. This shows that the dimensional stability of the composites increased with increasing content of Ni in the matrix. Similarly a decreasing trend in CTE was reported for the polyimide siloxane/Ni composite [15] and PVDF/clay [24]. In case of PVDF/clay, the addition of 5 wt% clay into the PVDF decreased the CTE approximately 50% [24]. It is probably due to the higher surface area to volume ratio and low CTE of the clay nano particles compared to that of Ni. The decrease in CTE of the PVDF/Ni composites may be attributed to lower intrinsic CTE of Ni ($13 \times 10^{-6}\text{ }^{\circ}\text{C}^{-1}$) [16] than that of pure PVDF ($195 \times 10^{-6}\text{ }^{\circ}\text{C}^{-1}$). In addition, the volume fraction of the loosely bound polymer gradually transforms to tightly bound polymer with increasing Ni content, which in-turn suppresses the thermal expansion of the composites [18]. Fig. 9 also correlates the experimental CTE with the values predicted from the rule of mixtures (RoM), which serves as the first order approximation to overall calculation of CTE of the composite. The experimental CTEs are slightly higher than those of predicted from the RoM indicating that the interaction between the matrix and the Ni particle is not strong. It has been well studied that good interaction between the matrix and the fillers (or particles) results in

CTEs lower than the values predicted from the RoM [18]. In present case, probably poor adhesion between the PVDF matrix and the Ni particles were not able to restrict the PVDF molecules from the expansion, in proportion of their volume fractions.

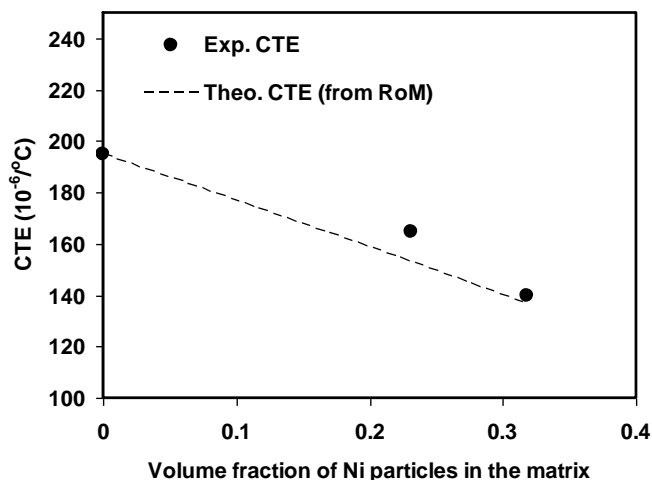


Fig. 9. Theoretical and experimental CTE as a function of Ni content.

Thermo gravimetric analysis (TGA)

The TGA was carried out to study the effect of Ni particles on the thermal stability and char yield of pure PVDF and its composites. Fig. 10(a) shows the residual weight of PVDF/Ni composites as a function of temperature in N_2 atmosphere.

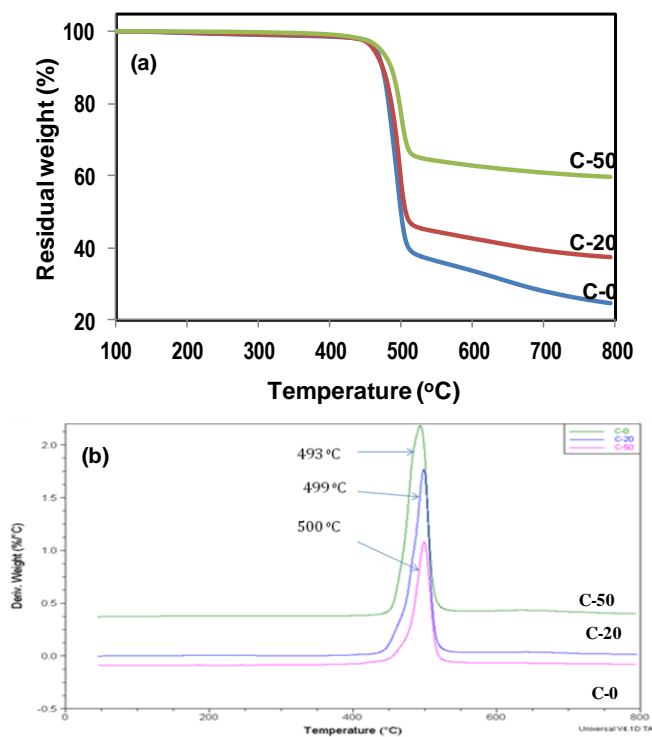


Fig. 10. (a) TGA curves and (b) DTG curves of PVDF/Ni composites in N_2 atmosphere.

The temperature of 10 wt% loss was considered as the degradation temperature (T_{10}). The values of T_{10} , maximum decomposition temperature (T_{max}) and char yield measured

at 800 °C are given in **Table 2**. It is observed that the pure PVDF is stable up to approximately 440 °C and its T_{10} is 473 °C. The T_{10} of the C-50 composite increased to about 485 °C indicating that the thermal stability of the composites increases with increasing content of Ni in the matrix. This is probably due to the higher heat capacity (125.58 J/g. °C) of Ni compared to that of pure PVDF (i.e., 1.5 J/g. °C) which causes preferable absorption of heat by the Ni particles [25-26]. The char yield is increased from 24.8 % for pure PVDF to 59.8 % for C-50 composite which again indicates that composites are thermally more stable than pure PVDF. **Fig. 10(b)** shows the derivative thermo gravimetric (DTG) thermograms of the composites. The maximum decomposition temperature (T_{max}) increased from 493 °C for pure PVDF to 500 °C for C-50 composite.

Table 2. Thermal properties (determined from TGA/DSC) of PVDF/Ni composites.

Sample codes	Data extracted from TGA/DTG curves			Data extracted from DSC curves					
	T_{10} (°C)	T_{max} (°C)	Char yield (%)	T_m	T_c	T_{on}	ΔH_c	χ_c	
C-0	473	493	24.8	163.95	130.77	138	33.39	31.89	
C-20	475	499	37.5	166.85	130.77	139	54.54	65.11	
C-50	485	500	59.8	163.53	134.99	141	26.52	50.66	

Differential scanning calorimetry (DSC)

Fig. 11 shows the second heating and first cooling curves of DSC for the C-0, C-20 and C-50 composites. The percent crystallinity (χ_c) of PVDF constituent of the composites was calculated using Eq. (5).

$$\chi_c = \frac{\Delta H_c}{W \Delta H_c^0} \times 100 \quad (5)$$

where, ΔH_c is the heat of crystallization, ΔH_c^0 is the heat of crystallization for 100 % crystalline PVDF (104.7 J/g) [13] and W is the mass fraction of PVDF in the composites. From the recorded heating and cooling curves, thermal properties were calculated and tabulated in the **Table 2**. It can be seen from the **Table 2** that the melting temperature and the onset temperature of crystallization are affected slightly with increasing content of Ni in the matrix. A similar trend in T_m was reported recently for AlN (5 μ m)/PEEK [27] and Al₂O₃ (8 μ m)/PEEK [28] composites. It is well known that the melting point of the polymer crystals is a function of lamellar thickness and degree of crystal perfection [29]. Therefore, a slight increase in T_m (of C-20), in present study, may be attributed to the increased crystal size and crystal perfection as confirmed from XRD. The increase in the crystallization temperature may be attributed to the heterogeneous nucleating effect of Ni particles. The crystallinity increased from 31.89 % for pure PVDF to 65 and 50.7 % for C-20 and C-50 composites, respectively. This is in agreement with the results obtained from XRD.

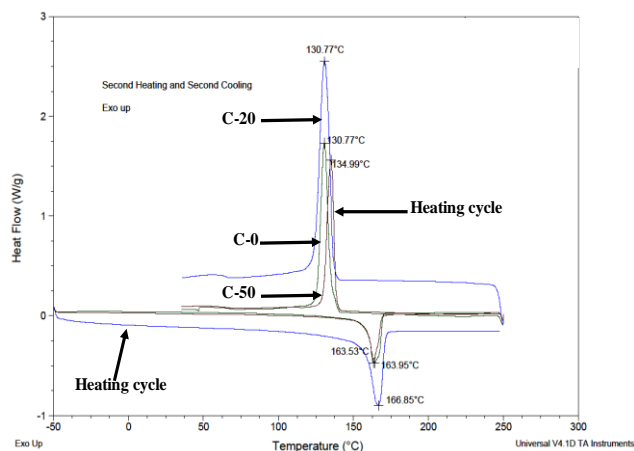


Fig. 11. Second heating and cooling cycles of DSC for PVDF/Ni composites

Electrical conductivity

Fig. 12a shows the electrical conductivity of pure PVDF and its composites as a function Ni content. The conductivity of pure PVDF is 6.3×10^{-13} S/cm and it increased with increasing content of Ni. A sharp increase of the conductivity was obtained between 20 wt% (or 4.8 vol%) and 40 wt% (or 11.8 vol%), i.e. it increased from about 6.2×10^{-11} to 1.8×10^{-3} S/cm. This indicates that the value of percolation threshold for present case is lower than those values reported elsewhere for metal-polymer composites [5-6, 13]. The lower value of percolation threshold may be attributed to the formation of high structure of Ni [30] and increased crystallinity of PVDF constituent in the composites as confirmed from the DSC. One more possible reason could be the processing route (i.e., solution mixing followed by hot pressing), which probably results in uniform distribution of Ni particles in the matrix and hence, form its thin 3-dimensional conductive network in the matrix. With lower percolation, the significant increased in conductivity for a semi-crystalline PVDF is very important for the application point of view. A similar trend was reported for Fe filled LDPE (crystallinity ~ 39%) and HDPE (crystallinity ~ 68%) composites, i.e., the values of percolation threshold for LDPE/Fe and HDPE/Fe composite were about 14-15 vol% and 12-20 vol%, respectively [9]. As the crystallinity of polymer increases, the volume of amorphous region of polymer decreases. The hard particles like Ni segregate in an amorphous region, thus give a lower value of percolation threshold than that of a polymer with fully amorphous. On the contrary, the percolation threshold for the CNF filled polymers increases with increasing crystallinity of the polymers. For example, the percolation threshold values for CNF filled polystyrene, LDPE and HDPE composites were 1.7, 2.4 and 14.3 vol% CNF, respectively. In such cases, crystalline regions of the polymers expel the CNF in the amorphous region of the polymer, thereby yielding aggregates of CNF and hence, results in higher percolation threshold [31]. In contrast, in present study, the aggregates of Ni particle formed thin chain-like structure of Ni particles which probably results in lower percolation threshold. On further increasing Ni content (i.e., above 11.8 vol%), the conductivity increases further approximately 2 orders of magnitude for C-70 composite indicating that

there is direct contact between Ni particles as seen in SEM images (**Fig. 6c**). The maximum conductivity of C-70 composite is 2.6×10^{-1} S/cm, which is approximately 2 orders of magnitude higher than the values reported by Xu et al. [15] for PVDF/Ni (2×10^{-3} S/cm at 33 vol% Ni) and PVDF/Zn composite (1.0×10^{-3} at 50 vol% Zn). Similarly, Li et al. [5] reported the maximum conductivity of 5×10^{-3} S/cm for 33 vol% Ni filled PVDF composites. In addition to good conductivity, the films have shown good flexibility.

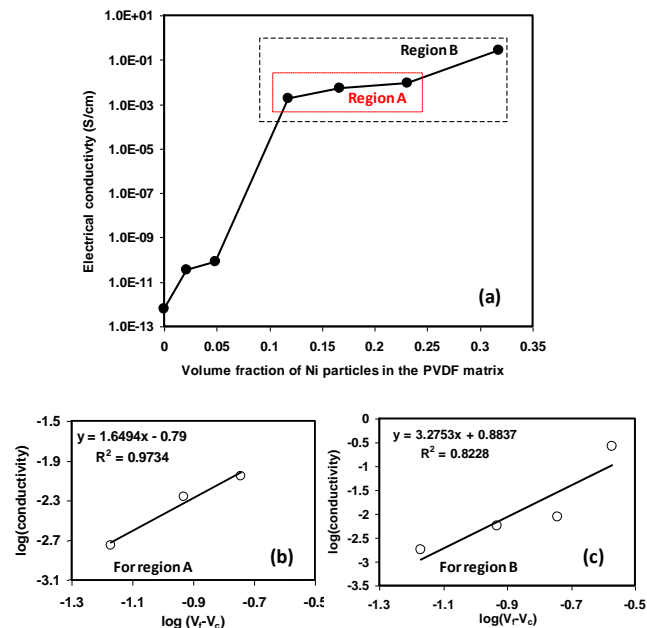


Fig. 12. Electrical conductivity for the PVDF/Ni composites as a function of Ni content (a), $\log \sigma_c$ versus $\log (V_f - V_c)$ for region A (b) and $\log \sigma_c$ versus $\log (V_f - V_c)$ for region B.

The dc electrical conductivity of the conductive polymer composites was correlated by a power law equation as represented by Eq. (6) [32-34].

$$\sigma_c = \sigma_0 (V_f - V_c)^t, V_f > V_c \quad (6)$$

where, σ_c is the conductivity of the composite, σ_0 is the conductivity of the Ni filler, V_f is the volume fraction of the Ni, V_c is the critical volume fraction of Ni at percolation threshold, and t is the critical exponent. In order to get an estimate for V_c and the critical exponent t , we fitted the conductivity data for $V_f > V_c$ to Eq. (6). Then the data were plotted in a $\log \sigma_c$ versus $\log (V_f - V_c)$ as shown in the inset of **Figs. 12 (b and c)**. This was done by variation of V_c in the interval from 0.05 to 0.09 in steps of 0.01 (see **Table 3**) for each value of V_c . The values of t and correlation factor (R^2) were determined from the slope of the linear relation of a log-log scale. It is interesting to see how the range of volume fraction (i.e., above V_c) of the conductive particle affect the value of t . When, volume fraction ranges from 0.1-0.2 (region A of **Fig. 12**), the value of $t=1.65$ is for a critical volume fraction of 0.05 (or 5 vol%) with a correlation factor (R^2) of 0.97. The value of $t=1.65$ is in excellent agreement with the theoretical universality value (1.6-2.0) of three dimensional systems [32-35]. However, when volume fraction ranges from 0.1-0.3 (region B of **Fig. 12**), the value of $t=3.28$ is for the same critical volume

fraction (i.e., 0.05). This means that the value of t also depends upon the composition range selected above the V_c . For a given system (in present case of PVDF/Ni) prepared under the similar processing conditions, the value of t increases for a wider range of composition than that of narrow range of composition. In contrast, for a single walled carbon nanotube (SCNT) filled polymer nanocomposite, its value is small for a wider composite range [35]. The higher value of t for the region B probably indicates change of electron transport phenomena from a tunneling to direct electron transfer between the Ni particles. As shown in the **Fig. 6(c)**, that the Ni particles formed a continuous 3-dimensional. However, it was well reported that fillers are generally have coating of insulating polymer matrix which hinder the direct contact between the fillers. Under the processing pressure of 45 MPa, PVDF matrix can easily deformed, hence the Ni-particles come together and the electrons can leap from the irregularities of one particle to the irregularities of others without any need for direct contact [36]. The percolation threshold value of the present case, to the best of our knowledge, is about three times lower than the values reported for any other metal filled polymer composites [5, 6, 13]. The lower critical volume fraction would be beneficial for the industries because higher volume fraction leads to the poor processability and mechanical properties [15]. In addition, the highest achieved electrical conductivity is 0.26 S/cm for the composite containing 32 vol% Ni with good flexibility, which is more than 50 times higher than that of reported by Li et al. [5] for a same Ni content. In addition to good electrical conductivity, the films have good flexibility, thermal stability and dimensional stability. The conductivities of these composites are better and comparable than those of required for antistatic (10^{-4} - 10^{-8} S/cm) and EMI shielding (> 1.0 S/cm) applications, respectively.

Table 3. Values of exponent constant and regression obtained from a power law.

Critical volume fraction (V_c)	Values from region A		Values from region B	
	R^2	t	R^2	t
0.05	0.97	1.65	0.82	3.28
0.06	0.977	1.50	0.81	2.99
0.07	0.983	1.34	0.80	2.69
0.08	0.988	1.17	0.78	2.38
0.09	0.999	0.997	0.75	2.05

Conclusion

Polymer matrix composites based on PVDF as matrix and Ni particle as reinforcement were successfully prepared using solution method followed by hot pressing. SEM showed uniform dispersion and 3-dimensional network of the Ni particles in the matrix. XRD and FTIR confirmed the presence of prominent α -phase of PVDF in the composites. The CTE of the composites decreased approximately 30% and the experimental CTEs are slightly higher than the values predicted from the rule of mixtures indicating poor interaction between the Ni particles and the matrix. The

thermal stability, char yield and the crystallinity of the composites increased significantly. The percolation threshold was found to be 5 vol% Ni where conductivity increased approximately 8 orders of magnitude, i.e., from 8.2×10^{-11} to 1.8×10^{-3} S/cm. The highest achieved electrical conductivity was about 0.26 S/cm, which is more than 50 times higher than those of reported in the literature for the same Ni content. This is because of the formation of a conductive network of Ni particles in the matrix. It was also investigated that the value of critical exponent (t) depends upon the composition range selected above the critical volume fraction and its value was found to decrease when the selected critical volume fraction is more. In addition to the better thermal and electrical conductivity, composites showed good flexibility.

Acknowledgements

The authors acknowledge the help of Dr. Govind, Scientist, C-MET, Pune for the measurement of particle size distribution of powder and Mr. Shinde, Department of Physics, University of Pune for SEM analysis. The department of Metallurgical Engineering and Materials Science, IIT Bombay, Mumbai, India is also acknowledged for providing XRD facility for the research.

Reference

1. Bagwell, R.M.; McManaman, J.M.; Wetherhold, R.C.; *Compos. Sci. Technol.* **2006**, 66, 522.
DOI: [10.1016/j.compscitech.2005.06.005](https://doi.org/10.1016/j.compscitech.2005.06.005)
2. Goyal, R.K.; Kambale, K.R.; Nene, S.S.; Sudhir, S.; Mulik, U.P. *Mater. Chem. Phys.* **2011**, 128, 114.
DOI: [10.1016/j.matchemphys.2011.02.065](https://doi.org/10.1016/j.matchemphys.2011.02.065)
3. Goyal, R.K.; Samant, S.D.; Thakar, A.K.; Kadam, A. *J. Phys. D: Appl. Phys.* **2010**, 43, 365404.
DOI: [10.1088/0022-3727/43/36/365404](https://doi.org/10.1088/0022-3727/43/36/365404)
4. Singh, V.; Kulkarni, A.R.; Ramamohan, T.R. *J. Appl. Polym. Sci.* **2003**, 90, 3602.
DOI: [10.1002/app.13085](https://doi.org/10.1002/app.13085)
5. Panda, M.; Srinivas, V.; Thakur, A.K. *Appl. Phys. Lett.* **2008**, 93, 242908.
DOI: [10.1063/1.3054163](https://doi.org/10.1063/1.3054163)
6. Panda, M.; Srinivas, V.; Thakur, A.K. *Appl. Phys. Lett.* **2008**, 92, 132905.
DOI: [10.1063/1.2900710](https://doi.org/10.1063/1.2900710)
7. Rothon, R.N. Rapra Tech. Ltd. **2001**, 12, 9.
8. Litchfield, D.W.; Baird, D.G. *Rheology Reviews.* **2006**, 1.
9. Lia, Y.J.; Xu, M.; Feng, J.Q.; Cao, X.L.; Yu, Y.F.; Dang, Z.M. *J. Appl. Polym. Sci.* **2007**, 106, 3359.
DOI: [10.1002/app.26988](https://doi.org/10.1002/app.26988)
10. Li, Y.J.; Xu, M.; Feng, J.Q. *Appl. Phys. Lett.* **2006**, 89, 072902.
DOI: [10.1063/1.2337157](https://doi.org/10.1063/1.2337157)
11. Li, Y.C.; Li, R.K.Y.; Tjong, S.C. *J. Nanomaterials* **2010**, 261748.
DOI: [10.1155/2010/261748](https://doi.org/10.1155/2010/261748)
12. Zhao, Z.; Yu, W.; He, X.; Chen, X. *Mater. Letter.* **2003**, 57, 3082.
DOI: [10.1016/S0167-577X\(02\)01440-4](https://doi.org/10.1016/S0167-577X(02)01440-4)
13. Xu, H.P.; Dang, Z.M. *Chem. Phys. Lett.* **2007**, 438, 196.
DOI: [10.1016/j.cplett.2007.02.076](https://doi.org/10.1016/j.cplett.2007.02.076)
14. Wu, G.; Zhang, C.; Miura, T.; Asai, S.; Sumita, M. *J. Appl. Polym. Sci.* **2001**, 80, 1063.
DOI: [10.1002/app.1191](https://doi.org/10.1002/app.1191)
15. Li, L.; Chung, D.D.L. *Composites* **1991**, 22, 211.
DOI: [10.1016/0010-4361\(91\)90321-7](https://doi.org/10.1016/0010-4361(91)90321-7)
16. ASM Metals Handbook (Vol. 2). Properties and selection: nonferrous alloys and special-purpose materials, 10th Ed. **1990**:1391-2.
17. Wu, J.; Chung, D.D.L. *J. Electron. Mater.* **2008**, 37, 1088.
DOI: [10.1007/s11664-008-0486-4](https://doi.org/10.1007/s11664-008-0486-4)
18. Goyal, R.K.; Tiwari, A.N.; Mulik, U.P.; Negi, Y.S. *J. Phys. D: Appl. Phys.* **2008**, 41, 085403.
DOI: [10.1088/0022-3727/41/8/085403](https://doi.org/10.1088/0022-3727/41/8/085403)
19. Priya, L.; Jog, J.P. *J. Polym. Sci. Part B: Polym. Phys.* **2002**, 40, 1682.
DOI: [10.1002/polb.10223](https://doi.org/10.1002/polb.10223)

20. Kim, J.W.; Cho, W.J.; Ha, C.S. *J. Polym. Sci. Part B: Polym. Phys.* **2002**, 40, 19.
21. Pejova, B.; Kocareva, T.; Najdoski, M.; Grozdanov, I. *Appl. Surf. Sci.* **2000**, 165, 271.
DOI: [10.1016/S0169-4332\(00\)00377-9](https://doi.org/10.1016/S0169-4332(00)00377-9)
22. Shah, D.; Maiti, P.; Gunn, E.; Schmidt, D.; Jiang, D.; Batt, C.; Giannelis, E. *Adv. Mater.* **2004**, 16, 1173.
DOI: [10.1002/adma.200306355](https://doi.org/10.1002/adma.200306355)
23. Xu, Y.; Chung, D.D.L.; Mroz, C. *Compos. A* **2001**, 32, 1749.
DOI: [10.1016/S1359-835X\(01\)00023-9](https://doi.org/10.1016/S1359-835X(01)00023-9)
24. Pramoda, K.P.; Mohamed, A.; Phang, I.Y.; Liu, T. *Polym. Int.* **2005**, 54, 226.
DOI: [10.1002/pi.1692](https://doi.org/10.1002/pi.1692)
25. Luyt, A.S.; Molefi, J.A.; Krump, H. *Polym. Degrad. Stab.* **2006**, 91, 1629.
DOI: [10.1016/j.polymdegradstab.2005.09.014](https://doi.org/10.1016/j.polymdegradstab.2005.09.014)
26. Jin, Z.; Pramoda, K.P.; Goh, S.H.; Xu, G. *Mater. Res. Bull.* **2002**, 37, 271.
DOI: [10.1016/S0025-5408\(01\)00775-9](https://doi.org/10.1016/S0025-5408(01)00775-9)
27. Goyal, R.K.; Tiwari, A.N.; Negi, Y.S. *Eur. Polym. J.* **2005**, 41, 2034.
DOI: [10.1016/j.eurpolymj.2005.04.009](https://doi.org/10.1016/j.eurpolymj.2005.04.009)
28. Goyal, R.K.; Tiwari, A.N.; Negi, Y.S. *J. Appl. Polym. Sci.* **2006**, 100, 4623.
DOI: [10.1002/app.23083](https://doi.org/10.1002/app.23083)
29. Bikiaris, D.N.; Papageorgiou, G.Z.; Pavlidou, E.; Vouroutzis, N.; Palatzoglou, P.; Karayannidis, G.P. *J. Appl. Polym. Sci.* **2006**, 100, 2684.
DOI: [10.1002/app.22849](https://doi.org/10.1002/app.22849)
30. Shui, X.; Chung, D.D.L. *J. Electron. Mater.* **1997**, 26, 928.
DOI: [10.1007/s11664-997-0276-4](https://doi.org/10.1007/s11664-997-0276-4)
31. Tjong, S.C.; Liang, G.D.; Bao, S.P. *Polym. Eng. Sci.* **2008**, 48, 177.
DOI: [10.1002/pen.20949](https://doi.org/10.1002/pen.20949)
32. Kirkpatrick, S. *Rev. Mod. Phys.* **1973**, 45, 574.
DOI: [10.1103/RevModPhys.45.574](https://doi.org/10.1103/RevModPhys.45.574)
33. Chen, G.; Weng, W.; Wu, D.; Wu, C. *Polym. J.* **2003**, 39, 2329.
DOI: [10.1016/j.eurpolymj.2003.08.005](https://doi.org/10.1016/j.eurpolymj.2003.08.005)
34. Wang, T.; Liu, J. *J. Electron. Manufact.* **2000**, 10, 181.
DOI: [10.1142/S0960313100000162](https://doi.org/10.1142/S0960313100000162)
35. Hu, N.; Masuda, Z.; Yan, C.; Yamamoto, G.; Fukunaga, H.; Hashida, T. *Nanotechnology* **2008**, 19, 215701.
DOI: [10.1088/0957-4484/19/21/215701](https://doi.org/10.1088/0957-4484/19/21/215701)
36. Lantada, A.D.; Lafont, P.; Sanz, J.L.M.; Munoz-Guijosa, J.M.; Otero, J.E. *Sensors and Actuators A* **2010**, 164, 46.
DOI: [10.1016/j.sna.2010.09.002](https://doi.org/10.1016/j.sna.2010.09.002)

Advanced Materials Letters

Publish your article in this journal

ADVANCED MATERIALS Letters is an international journal published quarterly. The journal is intended to provide top-quality peer-reviewed research papers in the fascinating field of materials science particularly in the area of structure, synthesis and processing, characterization, advanced-state properties, and applications of materials. All articles are indexed on various databases including DOAJ and are available for download for free. The manuscript management system is completely electronic and has fast and fair peer-review process. The journal includes review articles, research articles, notes, letter to editor and short communications.

